THE JOURNAL OF CHEMICAL PHYSICS VOLUME 59, NUMBER 10 15 NOVEMBER 1973

Emission spectra of solid rare-gas alloys

Aharon Gedanken, Baruch Raz, and Joshua Jortner
Department of Chemistry, Tel-Aviv University, Tel-Aviv, Israel

(Received 4 April 1973)

In this paper we present the results of an experimental study of the α-excited vacuum ultraviolet emission spectra of xenon–argon, xenon–krypton, krypton–argon, xenon–neon, krypton–neon, and argon–neon solid alloys in the temperature range 6–40 °K. Three mechanisms for electronic energy transfer to single impurity states and to impurity pairs were considered: (1) energy transfer from vibrationally relaxed homonuclear diatomic molecule of the host to Xe/Ar and to Xe/Kr impurity states; (2) energy transfer from the host vibrationally excited homonuclear diatomic molecule to Kr/Ar impurity states; and (3) energy transfer via impurity ionization or the formation of metastable states in neon alloys. The single impurity emission bands originating from the lowest Wannier states exhibit large red Stokes shifts reletive to the corresponding absorption bands, being close to the corresponding gas-phase transitions, and thus manifest the effect of medium relaxation around single impurity states. A similar effect is exhibited for diatomic molecules in pure solids and for excited impurity pairs. Qualitative information has been obtained regarding efficient nonradiative ralaxation processes between high Wannier impurity states. The emitting single impurity state involves in most cases the lowest lying, optically allowed, excited state. We have observed multiple trapping sites for the single impurity and for the impurity pairs in solid Ar and Kr but not in Ne. The population of these trapping sites is determined by the deposition temperature. Finally, spectroscopic evidence is obtained for the existence of heteronuclear rare-gas XeKr* and ArKr* diatomic molecules.

I. INTRODUCTION

The vacuum ultraviolet luminescence spectra of pure solid Ar, Kr, and Xe exhibit the emission from vibrationally relaxed, electronically excited rare-gas diatomic molecules, which result from an efficient exciton trapping process.[1,2] These broad structureless emission bands are analogous to emission of pure liquid Ne, Ar, Kr, and Xe and to the second continuum of rare gases excited at moderate pressures (> 100 torr) in the gas phase.[3] Solid Ne is unique in this respect as it exhibits a sharp emission band from the $n=1$ Wannier state (or in the language of the tight binding scheme the $^{1,3}P_1 \rightarrow {}^1S_0$ transitions).[4,5] The inhibition of the formation of Ne_2^* in solid Ne was attributed to inefficient vibrational relaxation for this diatomic molecule.[6] Vacuum ultraviolet emission studies of rare-gas alloys are of considerable interest and some work on this problem has been reported by Basov *et al.*[2] and very recently by Chesnovsky, Raz, and Jortner[7-9] and by Belov, Fugol, and Savchenko.[10] Previous work from this laboratory[7-9] on Xe/Kr liquid and solid alloys in the temperature range 120–80 °K has established the occurrence of extremely efficient electronic energy transfer from the host matrix to impurity atoms (or molecules). Thus reliable emission data for dense rare gas can be obtained only from ultrapure samples (total impurity content < 1 ppm).[7] In this paper we present the results of an experimental study of the vacuum ultraviolet emission spectroscopy of rare-gas alloys in the temperature range 6–50 °K. The goals of the present work can be summarized as follows.

(a) To establish the nature of electronic energy transfer from homonuclear diatomic rare gas molecules of the host matrix to rare-gas impurities in the solid alloys. At low impurity concentration (< 0.1%) energy transfer will occur to excited states of single impurities,[7] while at higher (> 0.1%) impurity concentrations, impurity pairs and higher aggregates will be excited indirectly. The major route for the host impurity electronic energy transfer is expected to take place from diatomic excited host molecules to the guest impurity states[7] via the Förster–Dexter mechanism.[11,12] This molecule-impurity atom energy transfer is deduced by long range dipole–dipole coupling, the transition probability being determined by the transition moments of the donor and of the acceptor and by the spectral overlap between the donor emission and the acceptor absorption spectra.[13,14] However, in cases where the spectral overlap is vanishingly small, other energy transfer mechanisms have to be considered.

(b) The excited states of a single isolated impurity in dilute rare-gas alloys are properly described in terms of a Wannier series.[15-17] As the conduction band in these solids is parabolic, the impurity absorption spectra exhibit hydrogenic series converging to the bottom of the conduction band. It is interesting to obtain information on which Wannier states are predominantly excited by electronic energy transfer.

(c) The emitting impurity state is not necessarily the Wannier level which was initially excited, as lower lying Wannier impurity states may be subsequently populated by nonradiative electronic relaxation processes. Information regarding these processes in simple solids will be of interest.

(d) To obtain further experimental information concerning exciton trapping and the nature of the resulting diatomic rare-gas molecules in these solids. While studies of pure gases[3] and condensed phases[1,2,7,9] have unambiguously established the formation of homonuclear excited diatomic rare-gas molecules, it is interesting to enquire whether in certain dense systems heteronuclear excited rare-gas diatomics are amenable to experimental observation.

(e) When an excited single impurity center does not form a heteronuclear diatomic molecule it will be interesting to obtain information regarding the Stokes shift between absorption and emission. Such data will be useful in assessing the nature of medium relaxation[7] around the impurity state.

(f) Energy transfer to impurity pairs at moderate impurity concentration may result in the formation of homonuclear diatomic impurity molecules. The observation of such impurity molecular emission is important for understanding medium induced vibrational relaxation of diatomic molecules. This problem is also interesting with respect to exciton trapping in the pure solids, in particular, for understanding the inhibition of the formation of Ne_2^* in solid neon.[6]

(g) Absorption spectroscopy of atomic and molecular impurity states in solid rare gases has established that in these systems the preparation method (in particular, the deposition temperature) can result in different trapping sites.[15,18,19] Complementary information concerning trapping sites from impurity emission will be crucial for unambiguous assignment of the nature of the emitting centers [see points (d), (e), and (f)].

II. EXPERIMENTAL PROCEDURES

The emission from solid rare-gas alloys bombarded with α particles was monitored by a 1 m spectrograph (McPherson 225) equipped with a gold coated grating (1200 lines per mm) blazed at 800 Å. The spectral resolution in the range 600–2000 Å was 10 Å. The light was detected by a sodium salicylate coated Pyrex plate mounted in front of a EMI 9514S photomultiplier, which was cooled to 220 °K.

The solid samples were prepared by injecting the gaseous mixtures on the 0.5 mC Americium α source which was mounted on a helium flow cryostat and cooled down to 6–50 °K. The temperature could be continuously varied and kept constant within ±0.5 °K. The gaseous mixtures were injected through an injection nozzle on the cold source. Throughout the injection process the nozzle temperature was kept at 300 °K by a thermocoax heater.

Matheson research grade rare gases were used for the sample preparation. The total impurity content of the Ar gas was less than 0.1 ppm. The major impurity content of the Kr gas was 11 ppm Xe. The Xe gas (total impurity content less than 20 ppm) was used mostly as a low concentration (~1%) impurity in other rare gases.

The gaseous mixtures were prepared in a vacuum system which was pumped to an initial pressure of less than 10^{-6} torr. The gaseous mixture was then injected on the cooled source, where the measured pressure in the spectrograph chamber prior to the injection was 2×10^{-7} torr. Ne matrices were deposited and measured at 6±2 °K, while Ar, Kr, and Xe matrices were prepared and measured in the temperature range 6–30 °K. From optical absorption studies we have observed[19] an appreciable enrichment of the solid samples of (rare gas)/Ne (deposited at 6±2 °K) relative to the gas phase composition. The enrichment factor for the impurity was ~5–10. Xe/Ar and Kr/Ar matrices (deposited at 20 °K) and Xe/Kr deposited at 35 °K exhibited an enrichment factor of ~2, while no enrichment of the solid matrix relative to the gas phase composition is expected for these matrices when deposited at 6 °K. The sample compositions presented in the paper refer to the gas phase composition of the mixtures.

III. EXPERIMENTAL RESULTS

A. Emission from Pure Solids

Apart from the intrinsic interest in these spectra, the emission of pure rare-gas solids provides a crucial test for the samples and for the gas handling procedure. In Figs. 1–3 we display the emission spectra of pure solid Ar, Kr, and Xe, obtained at different deposition temperatures. For future discussion of energy transfer processes we have also outlined in these figures the positions of the maxima of the absorption bands of Wannier impurity states in each matrix.[12,15] These emission spectra exhibit the following features.

(a) A single broad emission band is observed in each of the heavy rare gases in the spectral region 1000–2000 Å, which is assigned to the molecular transitions $^{1,3}\Sigma_u \rightarrow {}^1\Sigma_g$ to the repulsive ground state. We have not observed the broad emission bands peaking at 2000 Å and at 2300 Å reported by Belov *et al.*[10] and attributed to ion–molecule emission. Our measurements were performed at low excitation doses, while Belov *et al.*[10] might have observed effects of radiation damage. It cannot be ruled out that these bands reported by Belov *et al.* originate from impurity emission.

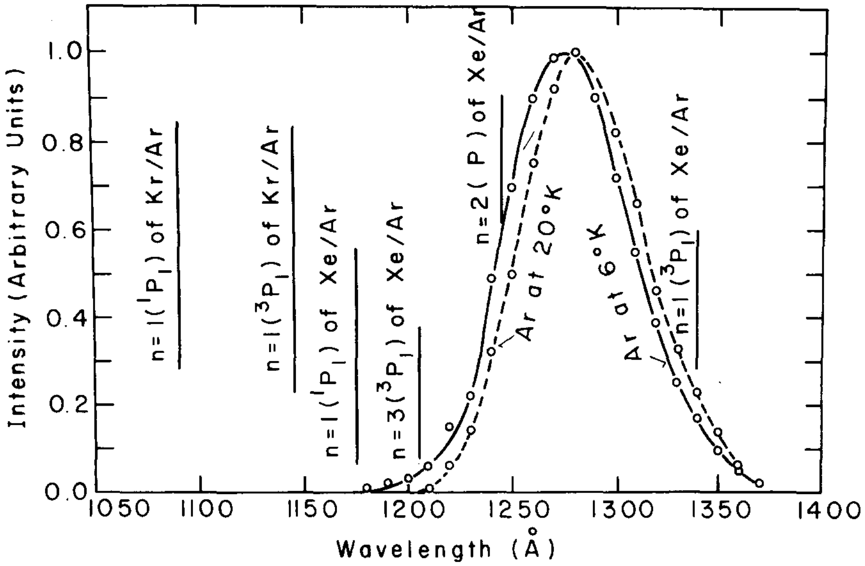

FIG. 1. Emission spectra of solid argon. The films were deposited and measured at 20 and at 6 °K. Absorption peak energies of krypton and xenon impurity states in solid argon are superimposed on the emission spectra.

(b) The present results for pure solid Ar (Fig. 1) concur with the original observation of Jortner *et al.*,[1] of Packard *et al.*,[4] and of Chesnovsky *et al.*[7] However, it should be noted that the present data are in variance with the recent observations of Belov *et al.*,[10] who besides the 1300 Å band have observed a broad emission peaking at 1600 Å in pure solid Ar. This emission, which was not observed by us, might originate from impurities, probably CO.

(c) The emission spectrum of solid krypton (Fig. 2) is characterized by a single band peaking at 1480 Å. The original observation of a shoulder at ~1600 Å in solid Kr(1) and the recent observation[2] of a shoulder at ~1520 Å originate from Xe impurity in the samples.

(d) The emission of pure solid Xe in the temperature region 40–6 °K is characterized (Fig. 3) by a single band peaking at 1720–1750 Å. This emission band is similar to those originally reported by Jortner *et al.*[1] and by Basov *et al.*[2] (at $T = 130-150\,^\circ K$). It should, however, be noted, that Basov *et al.*[2] have observed the buildup of another emission band peaking at 1640 Å which dominates the emission spectrum of solid Xe at 65 °K. A cursory examination of Basov's results for $T > 65\,^\circ K$ seems to be incompatible with the present data for $T < 40\,^\circ K$. However, we have recently observed that the temperature dependence of the emission spectrum of solid Xe is rather complex: The 1720 Å band at $T > 120\,^\circ K$ disappears with decreasing temperature while the 1640 Å band appears in the range 120–70 °K, while in the range 70–50 °K the 1640 Å band weakens and the 1720 Å band appears again. This interesting problem will be discussed elsewhere. Thus, the present observations for $T < 40\,^\circ K$ do not contradict Basov's original work.[2]

(e) The emission spectra of Xe_2^*, Kr_2^*, and Ar_2^* in the solid are qualitatively very similar to the second continuum of the rare gases in the gas phase[2,8] and to the emission in the corresponding liquids.[1,7,9] The small medium effect on the position and the line shape of the molecular emission bands is somewhat surprising, as these ${}^{1,3}\Sigma_u$ excited states are practically Rydberg states.[20] Absorption studies of extravalence atomic and molec-

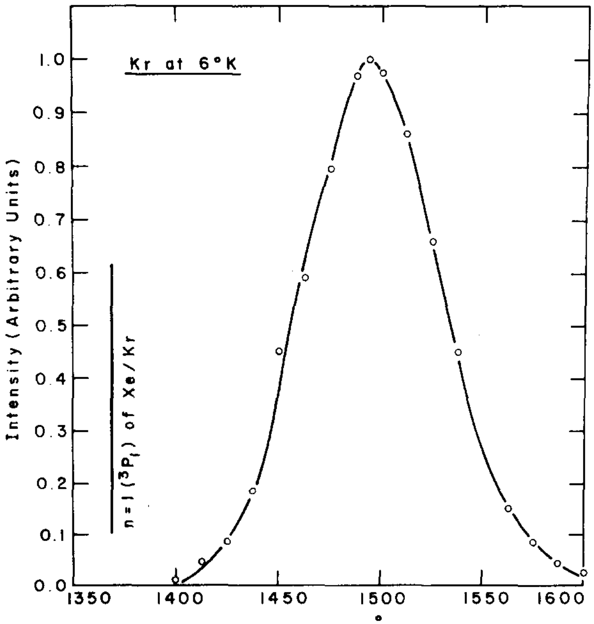

FIG. 2. Emission spectrum of solid krypton. Krypton film was deposited and measured at 6 ± 2 °K.

ular excitations in rare-gas solids have established the crucial role of overlap-orthogonality corrections which should result in an appreciable blue shift in absorption (which, for the rare-gas diatomics, can be observed only to highly excited vibrational levels). The emitting molecular impurity states are close to the emission bands in the gas phase. This effect originates from medium dilation around the localized extravalence molecular excitation.[7] In the case of Ar$_2^*$, Kr$_2^*$, and Xe$_2^*$ in the corresponding solids the medium relaxation results in practical cancellation of medium effects on the emission spectra. Two medium effects should be considered: (1) temperature dependence of the band width which results from thermal excitation of the intra molecular vibrations[8]; (2) a small temperature effect on the position of the maximum of the molecular emission.

(f) The position of the maxima of the emission bands of Xe$_2^*$ (Fig. 3) and of Ar$_2^*$ (Fig. 1) exhibit a weak temperature dependence, shifting to higher energies at lower temperatures. The total shift is $\Delta h\nu = 0.08$ eV for Xe$_2^*$ in annealed Xe deposited at 41 °K and scanned in the range 41–6 °K. This temperature effect can result from different local crystal configurations around the excited molecule at different temperatures. Alternatively, the temperature dependence of the lattice parameters may affect the local crystal dilation surrounding the excited diatomic molecule. The second interpretation implies that the multidimensional medium-molecule configuration potential curves exhibit a weak temperature dependence.

(g) The linewidths of the emission bands of Ar$_2^*$ and of Kr$_2^*$ below 20 °K and of Xe$_2^*$ below 40 °K are temperature independent. We have previously established[8] the temperature dependence of the spectral distribution of these molecular emissions in the gas phase and in liquids at $T \sim 100$ °K, which originates from the thermal population of the molecular vibrational levels. For our low temperature spectra $kT \ll \hbar w$, where $\hbar w$ is the molecular vibrational frequency, and the linewidth should be temperature independent. The low temperature linewidths in the pure solids (Table I) are in good agreement with the values interpolated from the data of Chesnovsky *et al.*[8]

The emission spectrum of solid Ne (Fig. 4) exhibits a well-defined band peaking at 742 Å (16.70 eV) and a broad weak shoulder at 770 Å (16.10 eV). These results agree with the original observations of Packard *et al.*[4] However, our data do not concur with the recent work of Fogul *et al.*,[5] who have not observed the weak shoulder at 770 Å. The emission at 742 Å is assigned to the decay of the $n = 1$ Wannier state (or, alternatively, to the $^1P_1 \to {}^1S_0$ transition). The Stokes shift between absorption and emission from the $n = 1$ state is 0.9 eV (bringing the emission band very close to the atomic $^1P_1 \to {}^1S_0$ transition). Again the large red Stokes shift results from medium dilation. The broad shoulder at 770 Å is assigned to the radiative decay from high vibrational levels of the Ne$_2^*$ molecule. No emission from the vibrationally relaxed Ne$_2^*$ mole-

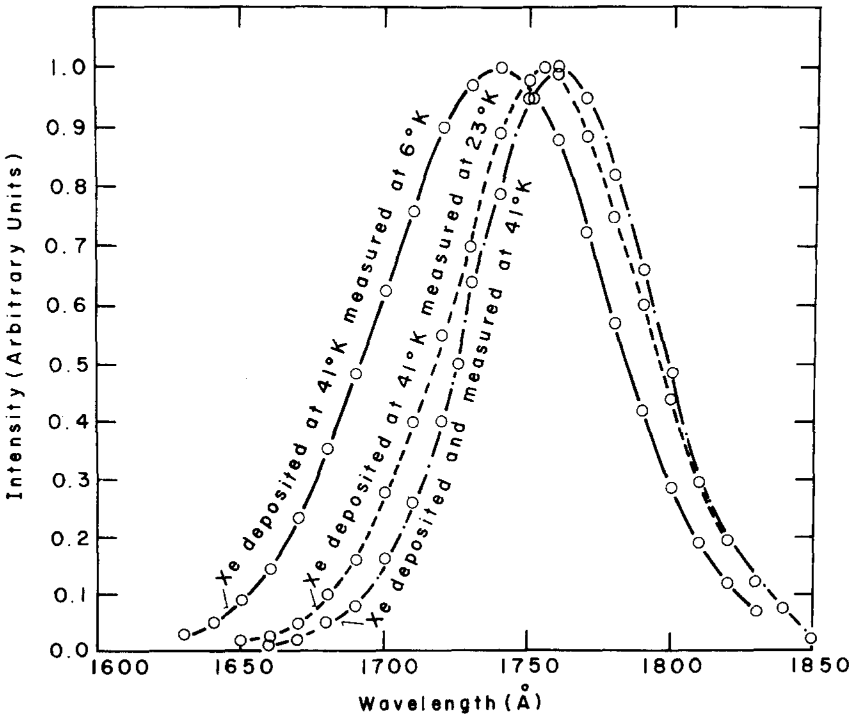

FIG. 3. Emission spectra of solid xenon. The films were deposited at 41 °K and measured at different temperatures.

TABLE I. Energies and linewidths for the second continuum emission of pure solid rare gases.

System	Peak energy (Å)	Linewidth (cm^{-1})
Solid Ar	1248	4300[a] 4570[b]
Solid Kr	1484	3150[a]
Solid Xe	1755	2500[a] 2550[b]

[a] This work at 6 °K.

[b] Data of Ref. (8) extrapolated to $T = 0$.

cule [which, in the gas phase, peaks at 880 Å (14.08 eV)][21] was observed in the solid. The retardation of vibrational relaxation of Ne_2^* in solid Ne has been previously discussed by us.[6]

B. Xenon-Argon Alloys

The emission spectra of argon doped by xenon at various concentrations and deposition temperatures (Fig. 5 and Table II) exhibit the following features.

(a) The emission band at 1280 Å observed at low Xe concentrations is attributed to Ar_2^* emission. The intensity of this band reduces with increasing Xe concentration, exhibiting the effect of electronic energy transfer between the host and the impurity.[22] Energy transfer via dipole–dipole coupling[11,12] occurs predominantly to the $n = 2$ ($^2P_{3/2}$) and somewhat less effectively to the $n = 1$ ($^2P_{3/2}$) and to the $n = 1$ ($^2P_{1/2}$) impurity states, as is evident from the spectral overlap between the donor (Ar_2^*) emission and the Xe impurity acceptor absorption bands (see Fig. 1).

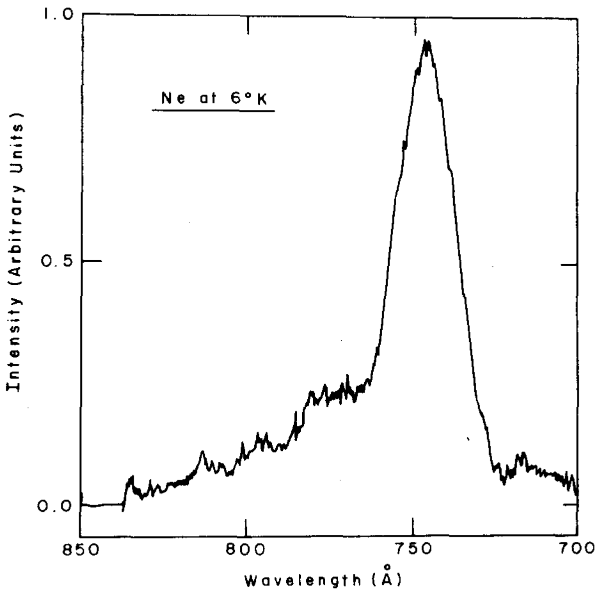

FIG. 4. Emission spectrum of solid neon. The film was deposited and measured at 6 ± 2 °K.

(b) The two emission bands peaked at 1475 ± 10 Å and at 1420 ± 10 Å are assigned to a single Xe impurity. The 1475 Å band has been previously observed in Xe/Ar thick crystals at 80 °K grown from the liquid.[7] This emission band, which is close to the $^3P_1 \rightarrow {}^1S_0$ transition in the gas phase, is attributed to the emission from the $n = 1$ ($^2P_{3/2}$) lowest Wannier state, where the medium has relaxed, resulting in the formation of a microscopic cavity surrounding the excited impurity center.[7] The relative intensities of the 1475 Å and the 1420 Å emission are sensitive to the deposition temperature (see Fig. 5). The most evident assignment of the 1420 Å band is that it involves a different single Xe impurity trapping site, where medium relaxation around the excited state is not efficient, so that the Xe emitting state is subjected to some overlap-orthogonality corrections, whereupon it is blue shifted relative to the atomic transition. Two alternative interpretations of the 1420 Å emission are rejected. First,

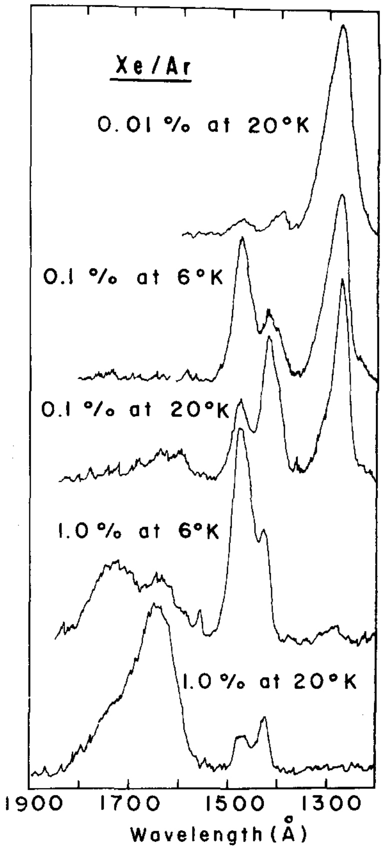

FIG. 5. Emission spectra of xenon doped argon solid mixtures. The concentrations outlined are the gas phase compositions. The mixtures were deposited and measured at 6 ± 2 and 20 °K.

TABLE II. Emission spectra of rare-gas alloys (sh means shoulder).

Xe/Ar 1%						Xe/Kr 1%						Xe/Ne 1%		
$T = 6$ °K			$T = 20$ °K			$T = 6$ °K			$T = 30$ °K			$T = 6$ °K		
Wavelength Å	Energy cm^{-1}	Intensity	Wavelength Å	Energy cm^{-1}	Intensity	Wavelength Å	Energy cm^{-1}	Intensity	Wavelength Å	Energy cm^{-1}	Intensity	Wavelength Å	Energy cm^{-1}	Assignment
												742	134 050	Ne $n = 1(^2P_{1/2})$
												1270	78 740	Xe $n = 1(^2P_{1/2})$
1280	78 125	1	···	···	···									Medium relaxed Ar_2^*
1430	69 930	3	1425	70 175	7									Medium relaxed Xe $n = 1(^2P_{3/2})$ site I
1480	67 570	10	1475	67 800	4	1465	68 260	4	1445	69 200	10	1465	68 260	Xe $n = 1(^2P_{3/2})$
						1560	64 100	10						Medium relaxed $KrXe^*$
1640	60 975	5	1645	60 790	10	1610	62 110	sh	1620	61 730	7			Xe_2^* site I
1725	57 970	6	1750	57 140	sh	1720	58 140	1	···	···	···	1725	57 970	Xe_2^* Medium relaxed

Kr/Ar 1%						Kr/Ne				Ar/Ne				
						0, 1%		1%		0, 1%		1%		
$T = 6$ °K			$T = 20$ °K			$T = 6$ °K		$T = 6$ °K		$T = 6$ °K		$T = 6$ °K		
Wavelength Å	Energy cm^{-1}	Intensity	Wavelength Å	Energy cm^{-1}	Intensity	Wavelength Å	Energy cm^{-1}	Wavelength Å	Energy cm^{-1}	Wavelength Å	Energy cm^{-1}	Wavelength Å	Energy cm^{-1}	Assignment
						750	133 330	···	···	748	133 690	···	···	Ne $n = 1(^2P_{1/2})$
										1070	93 460	1070	93 460	Ar $n = 1(^2P_{3/2})$
1135	88 105	4	1130	88 500	9									Medium relaxed Kr $n = 1(^2P_{3/2})$ site I
1200	83 330	1, 5	···	···	···									Kr $n = 1(^2P_{3/2})$
						1240	80 650	1240	80650					Medium relaxed Kr $n = 1(^2P_{3/2})$
1280	78 125	10	1280	78 125	10					···	···	1280	78 125	Medium relaxed Ar_2^*
1330	75 190	8	1340	74 630	9									Medium relaxed $KrAr^*$
1450	68 970	0, 2	1450	68 970	0, 5			1480	67570					Kr_2^* Medium relaxed

we do not assign this band to a XeAr* heteronuclear molecule because this emission was not observed in Xe/Ar gaseous mixture[8] and because under low temperature (6 °K) deposition conditions this band is weak. Second, we do not attribute this emission to excitonic diatomic impurity molecules (i.e., excited two Xe atoms separated by an Ar atom) since the 1420 Å emission is exhibited at low 0.01% impurity concentration. Our assignment of the 1420 and 1475 Å emission bands to different trapping sites of a single impurity is consistent with previous experience on absorption spectra of impurities in rare-gas solids.[15,18] Such evidence from emission spectroscopy in these systems was not yet reported. It should be, however, noted that the spectral shift between the two emission bands of Xe impurity observed herein is 0.33 eV, which is considerably larger than the difference between absorption bands attributed to different sites (~0.02 eV for benzene in rare gases[18] or ~0.1 eV for the "*A* band" of rare gases).[19] The large energy spacing between the two emission bands is consistent with the large Stokes shift between absorption and emission of the large radius Xe impurity state, whereupon small changes in the medium configuration surrounding the excited impurity state can go a long way in energetic modification of the impurity energy levels. Finally, we would like to point out that we were unable to observe the sharp band peaking at 1498 Å reported by Belov *et al.*[10] in Xe/Ar mixtures which should be observable under our conditions of spectral resolution.

(c) The two broad bands at 1720 and at 1640 Å observed at relatively high Xe concentration (see Fig. 5) are assigned to emissions from the Xe_2^* diatomic impurity molecule resulting from energy transfer to Xe pairs or aggregates. The relative intensities of these two bands are again sensitive to the deposition temperature. At low (6 °K) deposition temperature the 1720 Å band is intense, while at higher (20 °K) temperature the 1640 Å band dominates. This pattern is similar to that observed for the 1475 and the 1420 Å single impurity states. The 1720 Å band is assigned to the emission from the vibrationally relaxed Xe_2^* $(^{3,1}\Sigma_u)$ molecule where the surrounding medium has relaxed, so that the medium perturbations on its energy levels are small, as is the case in pure solid Xe at low temperatures (see Sec. II). Several possible assignments for the 1640 Å band should be considered.

(1) Emission from ArXe* heteronuclear diatomic molecule. This possibility is rejected as no analog emission is observed for Xe impurity in gaseous and liquid Ar.[7,8] Furthermore, the formation of such a molecule is expected to occur also at low Xe concentrations while our data indicate that for 0.01% and 0.1% (at 6 °K) Xe the emission in the 1600–1700 Å region is negligible.

(2) Competing emissions from $Xe_2(^1\Sigma_u)$ and $Xe_2(^3\Sigma_u)$ that occur at different energies (1640 and 1720 Å, respectively) and whose ratio is temperature dependent as suggested by Martin.[23] We do not accept this interpretation since the low temperature emission spectra reported herein are sensitive to the deposition temperature.

(3) A different trapping site results in retardation of vibrational relaxation of Xe_2^* and the 1640 Å emission results from vibrationally excited impurity molecule. Although we cannot entirely exclude this possibility, we are inclined not to accept it since the vibrational frequency of $Xe_2^*(^{1,3}\Sigma_u)$ is low ($\sim 140\ cm^{-1}$).[8] Thus vibrational relaxation effects should be efficient, as is evident from the emission of pure solid Xe at low temperatures (see Sec. II).

(4) The 1640 Å emission originates from the vibrationally relaxed Xe_2^* molecule located at a trapping site where the surrounding medium is not completely relaxed, whereupon the effects of nonorthogonality overlap corrections result in a blue shift relative to the "normal" 1720 Å molecular emission. This interpretation is consistent with the parallelism between the intensity of the 1640 Å molecular emission and the 1420 Å single impurity emission. We propose this interpretation, which provides the first example for large medium effect on the emission of rare-gas homonuclear molecule.

To conclude the discussion we have outlined in Fig. 6 the routes of electronic energy transfer, energy conversion, and radiative decay in the Xe/Ar solids. The experimental data are adequately interpreted on the basis of the following arguments: (a) efficient molecule-impurity energy transfer; (b) efficient nonradiative decay processes to the lowest optically allowed excited impurity state $n=1$ $(^2P_{3/2})$ (or $^3P_1$); (c) molecular formation at higher impurity concentration via a mechanism similar to that proposed for the gas phase; (d) the existence of two trapping sites for the single impurity and for the impurity pairs, where contributions are determined by the conditions of sample preparation.

C. Xenon–Krypton Alloys

The emission spectra of Xe/Kr solid mixtures (Fig. 7 and Table II) exhibit the following characteristics.

(a) A broad band peaked at 1450 ± 10 Å consists of a superposition of two emissions: (1) the Kr_2^* normal luminescence as exhibited by pure Kr and (2) the luminescence from the Xe $n=1$ $(^2P_{3/2})$ (or $^3P_1$) single impurity state. At 1% Xe the 1450 Å is

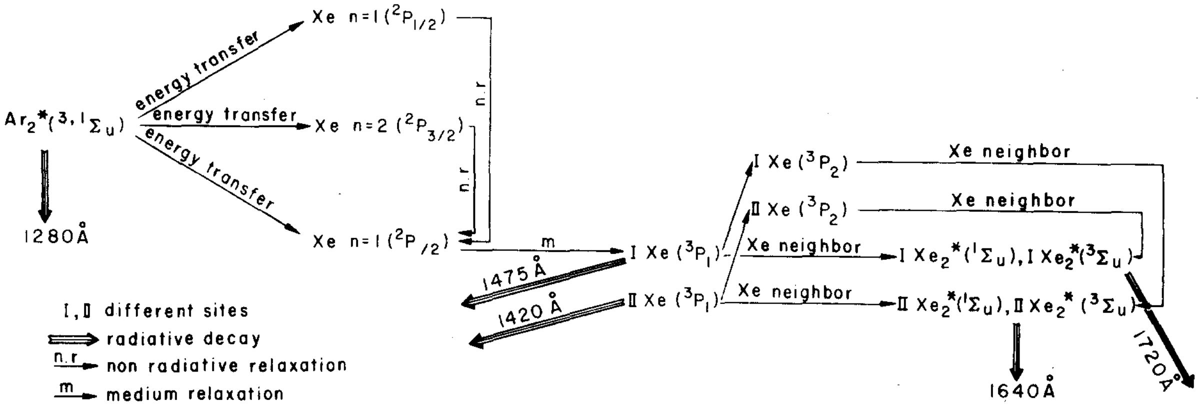

FIG. 6. A diagramatic scheme for the routes of electronic energy transfer, energy conversion, and radiative decay in the Xe/Ar solid mixtures.

appreciably narrower and shifted to higher energy as compared with the Kr_2^* emission (see Fig. 8), supporting its assignment as originating from the single impurity state.

(b) A broad emission band at 1570 Å. This band was previously reported by Basov *et al.*[2] in solid Xe/Kr, by Cheshnovsky *et al.*[7] in liquid and solid Xe/Kr alloys, and by Belov *et al.* in solid Xe/Kr.[10] Furthermore, an analogous emission band peaked at 1530 Å is observed in the luminescence of gaseous Xe/Kr mixtures.[18] This band is assigned to emission from the heteronuclear XeKr* diatomic molecule on the basis of the following arguments: (1) An analogous emission is observed in liquids and gaseous mixtures[9,18] and (2) this emission is exhibited at low 0.1% Xe concentrations, where impurity aggregation effects are negligible.

(c) The bands peaking at 1620 and at 1720 Å are assigned to emission from Xe_2^*. These emission bands are observed at relatively high ~1% Xe concentration and the high energy (1640 Å) band is favored at lower deposition temperatures. This behavior is analogous to that observed for the 1640 and 1720 Å bands in Xe/Ar mixtures (see Sec. IIIB). We again assign the 1720 emission to the "normal" Xe_2^* emission where the medium surrounding the impurity molecule is relaxed. The 1620 Å band is assigned to Xe_2^* located at another

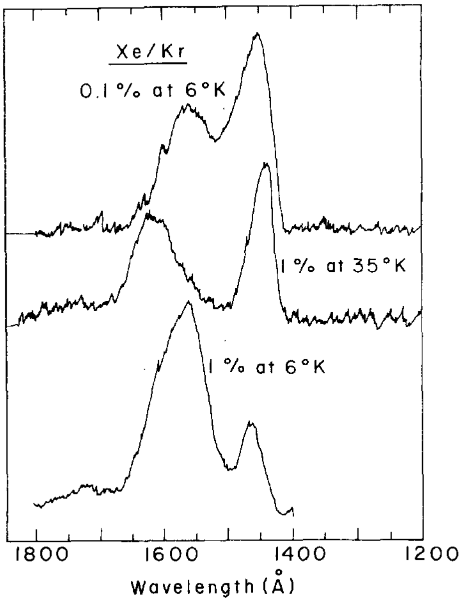

FIG. 7. Emission spectra of xenon doped krypton solid mixtures. The concentrations are the gaseous phase composition. Films were deposited and measured at 35 and 6 ± 2 °K.

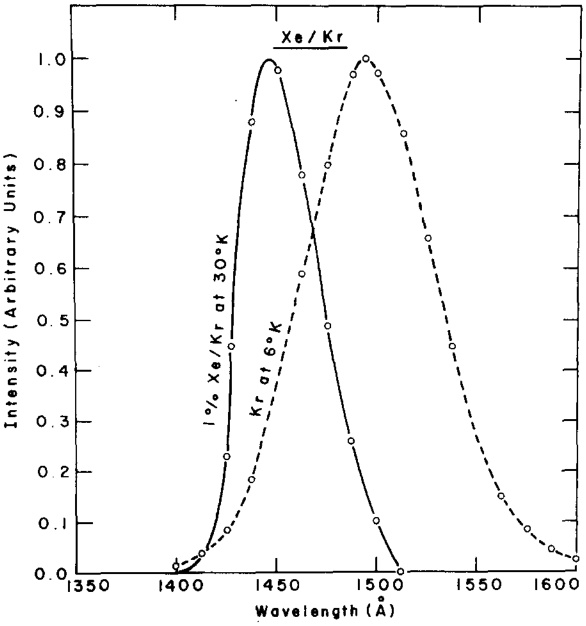

FIG. 8. Comparison between the 1450 Å emission of Xe/Kr and the emission from pure Kr.

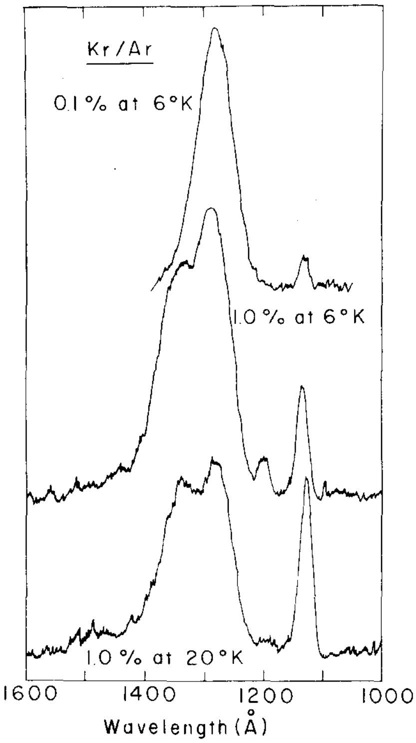

FIG. 9. Emission spectra of krypton doped argon solid mixtures. The concentrations are the gaseous phase composition. Films were deposited and measured at 20 and 6 ± 2 °K.

trapping site where large medium relaxation is not energetically feasible.

Energy transfer in the Xe/Kr system occurs from the host diatomic molecule to the impurity $n = 1$ ($^3P_{3/2}$) state. However, in view of the poor overlap between the host emission and the impurity absorption bands (see Fig. 2) the efficiency of the electronic transfer process is expected to be lower than in the Xe/Ar system. An alternative inefficient pathway of electronic energy transfer may involve highly vibrationally excited levels of the host Kr_2^* molecule, where energy transfer competes with vibrational relaxation.

D. Krypton–Argon Alloys

The emission spectra of Kr/Ar mixtures (Fig. 9 and Table II) exhibit the following characteristics.

(a) An emission band at 1280 Å is assigned to the host Ar_2^* emission.

(b) The emission band at 1135 Å is assigned to the decay of the $n = 1$ ($^2P_{3/2}$) impurity state. This is the prominent impurity emission in the system. At low deposition temperatures a weak band at 1200 Å is observed which is assigned to a second trapping site of the single impurity. Surprisingly enough, the 1135 Å band is considerably blue shifted relative to the free atomic emission (1240 Å), so that medium relaxation is more efficient around the impurity site that gives rise to the 1200 Å emission.

(c) The broad emission at ~1450 Å is assigned to the "normal" Kr_2^* emission from vibrationally relaxed molecules in a medium relaxed site.

(d) The emission band at 1330 Å observed at high (1%) impurity concentration cannot be unambiguously assigned, and two possibilities should be considered: (1) This band originates from a second trapping site for the Kr_2^* impurity molecule, which is blue shifted relative to the "normal" 1450 Å emission, (2) this emission is due to the ArKr* heteronuclear molecule, as also proposed by Belov *et al.*[10] We prefer the second interpretation because an analogous emission peaking at 1350 Å has been observed by us for Kr/Ar gaseous mixtures.

As is evident from Fig. 1 there is no overlap between the host Ar_2^* emission band and the absorption bands of the Kr guest impurity states. Thus electronic energy transfer does not occur from the vibrationally relaxed host diatomic molecule. In this case energy transfer can take place from the lower host exciton states and from the vibrationally excited levels of Ar_2^*, whereupon electronic energy transfer competes with intramolecular vibrational relaxation of Ar_2^*, making the former process relatively inefficient.

E. Solid Neon Alloys

The emission spectra of Xe/Ne, Kr/Ne, and Ar/Ne (Figs. 10–12) reveal the following emissions.

(a) The Ne host emission from the $n = 1$ exciton level (or $^1P_1 \rightarrow {}^1S_0$ transition) at 743 Å.

(b) The guest emission from single impurity states are located at 1070 Å for Ar, 1240 Å for Kr, and at 1270 Å and 1465 Å for Xe. The Ar and Kr

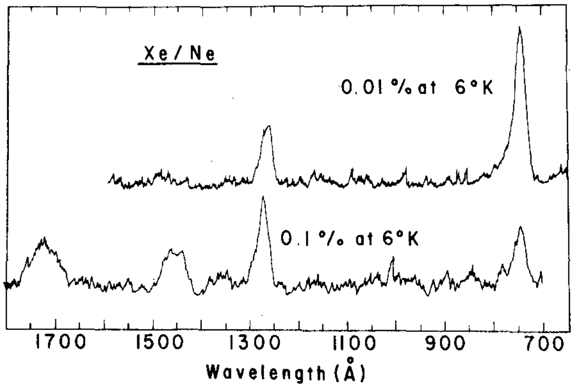

FIG. 10. Emission spectra of xenon doped neon solid mixtures. The films were deposited and measured at 6 ± 2 °K.

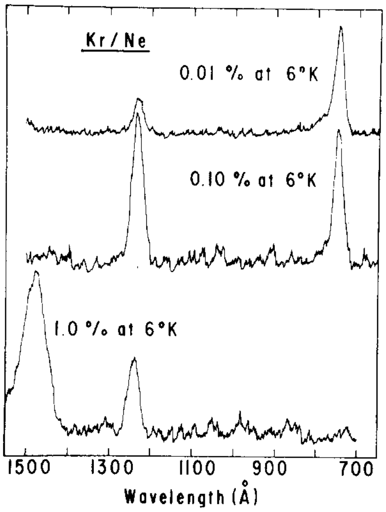

FIG. 11. Emission spectra of krypton doped neon solid mixtures. The films were deposited and measured at 6 ± 2 °K.

bands are very close to the $^3P_1 \to {}^1S_0$ free atom emissions. The two Xe bands again practically coincide with the $^1P_1 \to {}^1S_0$ and with the $^3P_1 \to {}^1S_0$ atomic gas phase transitions. The single atomic impurity emissions exhibit large red Stokes shifts relative to the corresponding impurity absorption bands, revealing again the effects of medium dilation around the excited center. The single band observed in each of the Ar and Kr alloys is assigned to decay from the $n = 1$ ($^2P_{3/2}$) [or the ($^3P_1$) atomic state], while the two bands in the Xe alloys are assigned to emission from the $n = 1$ ($^2P_{3/2}$) and $n = 1$ ($^2P_{1/2}$), or alternatively from the $^3P_1$ and $^1P_1$ states.

(c) At high (1%) impurity concentration, impurity molecular bands are observed at 1725 Å for Xe$_2^*$, 1480 Å for Kr$_2^*$, and 1280 Å for Xe$_2^*$. These "normal" molecular emissions exhibit again the effects of efficient medium relaxation around the excited diatomic molecule.

From the experimental point of view it is important to notice that in solid Ne we have not observed the occurrence of different trapping sites for the atomic and the molecular impurity states. This observation concurs with previous absorption studies which have established that solid Ne is a "soft" or "self-annealing" matrix, in view of its low melting point.[24]

Host–guest electronic energy transfer in solid Ne is drastically different from that encountered in the other rare-gas alloys. In this system the energy of the $n = 1$ matrix state is considerably higher than the onset of the transition from the impurity to the conduction band. The impurity band gap E_g, i.e., the ionization potential of an impurity in the solid matrix, is given by[19] $E_g = I_g + P_+ + V_0$, where I_g is the gas phase ionization potential of the impurity, P_+ corresponds to the medium polarization energy by the positive hole, and V_0 represents the energy of the bottom of the matrix conduction band (relative to the vacuum level). For solid Ne, $V_0 = +0.5$ eV,[25] so that $P_+ + V_0 \simeq 0$ and $E_g \simeq I_g$. The gas phase ionization potentials[26] of Ar, Kr, and Xe are lower than the $n = 1$ state of solid Ne.[24,27] This electronic energy transfer from the matrix can occur by two mechanisms: (1) ionization of the impurity to the conduction band followed by electron hole recombination to electronically excited impurity states and (2) excitation of metastable impurity states above the onset of the conduction band. These metastable excited states can decay by autoionization to the conduction band, followed by the route outlined in (1), or alternatively, decay nonradiatively to lower band excited states. The branching ratio between nonradiative decay of metastable states and autoionization together with direct ionization can be monitored from photoconductivity studies.

Finally we have to point out that in high concentration (1%) Xe/Ne mixtures, the effects of direct excitation of the Xe impurity are important because of the high ratio of the nuclear charges. This may be the reason for the appearance of the 1470 Å emission in Xe/Ne at 1% Xe.

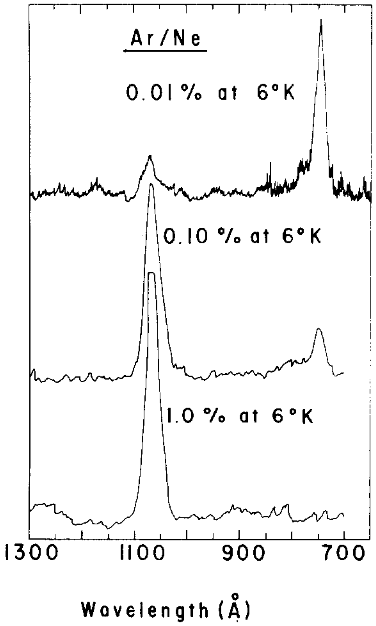

FIG. 12. Emission spectra of argon doped neon solid mixtures. The films were deposited and measured at 6 ± 2 °K.

F. Efficiency of Electronic Energy Transfer

In the Xe/Ar and Xe/Kr systems electronic energy transfer occurs from vibrationally relaxed donor diatomic molecule (Ar_2^* or Kr_2^*) to the impurity Wannier states. On the other hand, in the Kr/Ar system electronic energy transfer will occur from the host low exciton state and from vibrationally unrelaxed Ar_2^* molecule. We thus expect the efficiency of energy transfer in the Kr/Ar system to be low in view of competition between energy transfer and vibrational relaxation of the above molecule. To provide a semiquantitative basis for this argument we shall utilize the Förster–Dexter energy transfer theory via dipole–dipole coupling.[11,12] The quantum yield for the donor emission η in the presence of concentration C of the acceptor is given by[28]

$$\eta/\eta_0 = 1 - \pi\sqrt{q}\,\exp(q^2)[1-\mathrm{erf}(q)]\,, \tag{1}$$

where $\eta = \eta_0$ at $C = 0$, while $q = \frac{1}{2}\sqrt{\pi}\,C/C_0$, in which the reduced concentration

$$C_0 = 3/4\pi R_q^3 \tag{2}$$

is expressed in terms of the critical transfer radius where the probability of the radiative decay of the acceptor is equal to the energy transfer probability. Invoking second order perturbation theory we have[11]

$$R_q = (\lambda^3 \mu_A^2 F/8\pi^2)^{1/6}\,, \tag{3}$$

where λ is the (mean) wavelength for the acceptor emission, μ_A the transition moment for the acceptor absorption, while F represents the spectral overlap

$$F = \int f_{Aa}(E) f_{De}(E)\,dE \tag{4}$$

between the (normalized) acceptor absorption $f_{Aa}(E)$ and the donor emission $f_{De}(E)$ line shapes. It should be noted that R_q exhibits a weak dependence on F.

From the experimental data for Xe/Ar and Kr/Ar mixtures deposited at 6 °K (where sample enrichment effects are small), we have calculated the ratios I_A/I_D between the total emission intensity of the acceptor (which for 0.1%–0.01% Xe/Ar corresponds to the sum of the 1430 and 1470 Å bands, while for 0.1% Kr/Ar it is given by the 1130 Å band) and the emission intensity of the donor (the 1280 Å band for Xe/Ar and for Kr/Ar). This intensity ratio corresponds to $I_A/I_D = (\eta_0 - \eta)/\eta$. The resulting R_q values (Table III) demonstrate the relative efficiency of the energy transfer process in the Xe/Ar system where the spectral overlap function [Eq. (4)] is expected to exceed [see Eq. (3)] F for the Kr/Ar system by about a numerical factor of 36. Thus the efficiency of energy transfer, which is determined by R_q^3 [see Eqs. (1) and (2)] is smaller for energy transfer competing with vibrational relaxation by about two orders of magnitude.

IV. CONCLUDING REMARKS

In his basic theoretical study of the electronic states of homonuclear rare-gas molecules, Mulliken[20] has stated that "correlations of the condensed phase spectra with the gas spectra are not easy." On the basis of the experimental data presented herein we are inclined to agree that the emission spectra of dense rare gases are rather complicated. We hope, however, that our experimental results elucidate several important radiative and nonradiative decay channels of single impurity Wannier states and of excited impurity pairs in deep gas insulations. Our main conclusions can be summarized as follows.

A. Electronic Energy Transfer Mechanisms

Three mechanisms for host-impurity electronic energy transfer were considered: (1) Energy transfer from the vibrationally relaxed and medium relaxed host diatomic molecule to impurity states (Xe/Ar, Xe/Kr). This mechanism was previously considered for analogous processes in the gas phase.[11] The only change introduced by the medium is the modification of the spectral overlap function [Eq. (4)]. (2) Energy transfer from vibrationally excited diatomic molecule to impurity states (Kr/Ar). (3) Energy transfer via impurity ionization or formation of metastable excitations (Ne alloys). The impurity ionization process to the conduction band bears a close analogy to Penning ionization in the gas phase, and is similar to the ionization of F centers by excitons in alkali halides.

B. Emission from the $n = 1$ Impurity Wannier State

The emission from the lowest Wannier state was observed for Xe/Ar, Xe/Kr, Kr/Ar, Ar/Ne, and Kr/Ne solids while emission from two spin orbit split $n = 1$ Wannier states was detected from the Xe/Ne alloys. These single impurity emission bands exhibit large red Stokes shifts and are close to the corresponding atomic transitions (see Table IV). Thus the effect of medium relaxation around single impurity states and diatomic impurity molecules is of great generality in these systems.

TABLE III. Critical radii for electronic energy transfer in rare-gas alloys.

System	I acceptor I donor	Rq (Å)
0.01% Xe/Ar	0, 10	18
0, 1% Kr/Ar	0, 05	6.0
1% Kr/Ar	0, 84	7.5

TABLE IV. Comparison between the emission of solid rare gases and of rare-gas alloys and the absorption of impurities states.

System	Emission peak in the solid (eV)	Absorption peak of impurity[a] in (eV)	Emission of the atom or molecule in the gaseous phase (eV)	Assignment[b]
Xe/Ar	8.40	9.22	8.43	Xe $n=1(^2P_{3/2})$
Xe/Kr	8.49	9.01	8.43	Xe $n=1(^2P_{3/2})$
Kr/Ar	10.33	10.79	10.03	Kr $n=1(^2P_{3/2})$
Xe/Ne	9.76	11.28	9.56	Xe $n=1(^2P_{1/2})$
Xe/Ne	8.48	9.08	8.43	Xe $n=1(^2P_{3/2})$
Kr/Ne	10.00	10.62	10.03	Kr $n=1(^2P_{3/2})$
Ar/Ne	11.58	12.50	11.61	Ar $n=1(^2P_{3/2})$
Xe_2^*/Xe	7.06	···	7.20	$Xe_2^*(^{1,3}\Sigma_u)$
Xe_2^*/Kr	7.20	···	7.20	$Xe_2^*(^{1,3}\Sigma_u)$
Xe_2^*/Ar	7.18	···	7.20	$Xe_2^*(^{1,3}\Sigma_u)$
Xe_2^*/Ne	7.18	···	7.20	$Xe_2^*(^{1,3}\Sigma_u)$
Kr_2^*/Kr	8.35	···	8.35	$Kr_2^*(^{1,3}\Sigma_u)$
Kr_2^*/Ar	8.55	···	8.35	$Kr_2^*(^{1,3}\Sigma_u)$
Kr_2^*/Ne	8.37	···	8.35	$Kr_2^*(^{1,3}\Sigma_u)$
Ar_2^*/Ar	9.65	···	9.65	$Ar_2^*(^{1,3}\Sigma_u)$
Ar_2^*/Ne	9.68	···	9.65	$Ar_2^*(^{1,3}\Sigma_u)$

[a] Reference (15).

[b] All emission refer to medium relaxed trapping site.

C. Nonradiative Transitions

In five out of the six alloys studied herein the emitting single impurity state involves the lowest (optically allowed) Wannier state. The population of these impurity states via electronic energy transfer does not result in exclusive population of this level (see Sec. IIIB). Thus nonradiative decay processes between high Wannier states are efficient on the time scale of their radiative decay. The only exception involves the Xe/Ne system where emission from the $n=1$ $(^2P_{1/2})$, i.e., $^1P_1$ state was observed. It will be interesting to invoke the theory of multiphonon relaxation processes[29] for a deeper theoretical understanding of these nonradiative transitions.

D. Multiple Trapping Sites

We have established the occurrence of multiple trapping sites for the single impurity and for the impurity pairs in solid Ar and in solid Kr, but not in solid Ne. One trapping site enables efficient medium relaxation around the impurity. The second site prohibits complete medium relaxation resulting in a blue shift of the emission band relative to the "normal" emission. The experimental evidence for multiple trapping sites, based on sensitivity to the deposition temperature, is quite strong.

On the basis of the present and previous[7,9] results we assert that the normal emissions which are close to the gas phase energy of the single impurity and of the impurity homonuclear molecule are well exhibited by three types of dense systems: (1) In the liquid mixtures. (2) In solid alloys grown from the melt and in solid Ne, when studied just below their melting temperature. It is known that under these conditions metastable crystalline structures and mixtures of metastable and stable structures (which are also very sensitive to small impurity content) are exhibited by the rare gases.[30] (3) In solid samples deposited at low (6 °K) temperatures. Under these conditions polycrystalline samples are produced. Thus our experimental results demonstrate that efficient medium relaxation occurs in trapping sites produced in "disordered type" dense phases in solid Ne, Ar, and Kr.

E. Heteronuclear Diatomic Rare-Gas Molecules

Spectroscopic evidence has been obtained for the existence of the KrXe* and possibly ArKr* heteronuclear rare-gas diatomics. In view of the pitfalls involved in the identification of molecular emission from multiple trapping sites, our evidence for these species mainly rests on the observation of analogous emission bands in the gas phase or in liquid alloys.

[1] J. Jortner, L. Meyer, S. A. Rice, and E. G. Wilson, J. Chem. Phys. **42**, 4250 (1963).

[2] (a) N. G. Basov, V. A. Danilychev, Yu. M. Popov, and D. D. Khodkevich, Zh. Eksp. Teor. Fiz. Pis'ma Red. **12**, X, 473 (1970) [JETP Lett. **12**, 329 (1970)]; (b) N. G. Basov, M. Balashov, C. V. Bogdankevich, V. A. Danilychev, G. N. Kashnikov, N. P. Latzov, and D. P. Khodkevich, J. Lumin. **1**, 834 (1970).

[3] R. E. Huffman, J. C. Larabee, and Y. Tanaka, Appl. Opt. **4**, 1581 (1965).

[4] R. E. Packard, F. Reif, and C. M. Surko, Phys. Rev. Lett. **25**, 1435 (1970).

[5] I. Ya. Fugol, E. V. Savchenko, and A. G. Belov, Zh. Eksp. Teor. Fiz. Pis'ma Red. **16**, 245 (1972) [JETP Lett. **16**, 172 (1972)].

[6] A. Gedanken, B. Raz, and J. Jortner, J. Chem. Phys. **59**, 1630 (1973).

[7] O. Cheshnovsky, B. Raz, and J. Jortner, J. Chem. Phys. **57**, 4628 (1972).

[8] O. Cheshnovsky, B. Raz, and J. Jortner, Chem. Phys. Lett. **15**, 475 (1972).

[9] O. Cheshnovsky, B. Raz, and J. Jortner, J. Chem. Phys. (to be published).

[10] A. G. Belov, I. Ya. Fugol, and E. V. Savchenko, Solid State Commun. **12**, 1 (1973).

[11] Th. Förster, Ann. Phys. (Leipz.) **2**, 55 (1948).

[12] D. L. Dexter, J. Chem. Phys. **21**, 836 (1953).

[13] A. Gedanken, J. Jortner, B. Raz, and A. Szöke, J. Chem. Phys. **57**, 3456 (1972).

[14] O. Cheshnovsky, B. Raz, and J. Jortner, J. Chem. Phys. **57**, 3456 (1973).

[15] G. Baldini, Phys. Rev. **137**, A508 (1965).

[16] J. Hermanson and J. C. Phillips, Phys. Rev. **150**, 652 (1966).

[17] The lowest excited impurity state of a rare gas can be described either in terms of the tight binding approximation involving large overlap–orthogonality corrections or by the Wannier Scheme with large central cell corrections. To specify these lowest spin orbit split stating states we shall use synonomously the notation $n = 1$ ($^2P_{3/2}$) and $n = 1$ ($^2P_{1/2}$) or $^3P_1$ and $^1P_1$.

[18] B. Katz, B. Sharf, M. Brith, A. Ron, and J. Jortner, Chem. Phys. Lett. **2**, 189 (1968).

[19] A. Gedanken, B. Raz, and J. Jortner, J. Chem. Phys. **58**, 1178 (1973).

[20] R. S. Mulliken, J. Chem. Phys. **52**, 5170 (1970).

[21] R. E. Huffman, J. C. Larrabee, and D. Chambers, Appl. Opt. **4**, 1145 (1965).

[22] The linewidth of the Ar_2^* emission at 1280 Å in low concentration 0.01% Xe/Ar solid fits well with the emission of pure Ar. At higher Xe concentration ∼ 0.1%, some indication of narrowing and blue shift of this band is observed. It could be tempting to assign this effect to the contribution of emission for Xe $n = 2$ ($^2P_{3/2}$) state. However, this interpretation has to be rejected on the basis of the observation that at 1% Xe the emission in this region is practically washed out, and has thus to be assigned to the host.

[23] M. Martin, J. Chem. Phys. **54**, 3289 (1971).

[24] E. Boursey, J. Y. Roncin, and H. Damany, Phys. Rev. Lett. **25**, 1279 (1970).

[25] B. Raz and J. Jortner, Chem. Phys. Lett. **9**, 222 (1971).

[26] C. E. Moore, *Atomic Energy Tables*, Natl. Bur. Std. (U.S.) (U.S. GPO, Washington, D.C., 1958).

[27] R. Haensel, G. Keilel, E. E. Koch, N. Kosuch, and M. Skibowski, Phys. Rev. Lett. **25**, 1281 (1970).

[28] K. B. Eisenthal and S. Siegel, J. Chem. Phys. **41**, 652 (1964).

[29] R. Kubo and Y. Toyozawa, Prog. Theor. Phys. **13**, 160 (1955).

[30] (a) L. Meyer, C. Barret, and P. Haasen, J. Chem. Phys. **40**, 2744 (1964); (b) L. Meyer, Adv. Chem. Phys. **16**, 343 (1969).